

# Updates on the ESSvSB Target Station potentialities for CP violation discovery

Julie Thomas, IPHC, Université de Strasbourg,  
CNRS/IN2P3, 67037 Strasbourg, France.

*On behalf of the ESSvSB Collaboration*

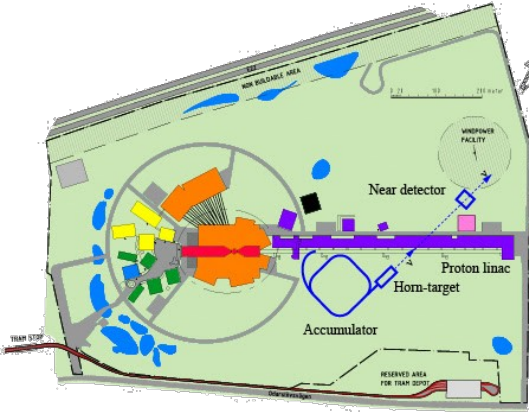


Fig. 1 : ESSvSB site in Lund

# The ESSvSB project [1]

CP violation in leptonic sector is a candidate to explain the asymmetry between matter and anti-matter observed in the Universe :  $P(\nu_i \rightarrow \nu_j) \neq P(\bar{\nu}_i \rightarrow \bar{\nu}_j)$ .

The ESS Neutrino Super Beam project proposes to use the linac of ESS<sup>[2]</sup> to produce a high-intensity and low-energy neutrino beam.

This combination of high intensity and low energy will allow to access the second maximum in the neutrino oscillation probability.

Facility parameters	
Proton beam kinetic energy (GeV)	2.5
Total beam power (MW)	5
Beam intensity (ppp)	$8.9 \times 10^{14}$
Beam pulse duration Linac / accumulator (ms/ $\mu$ s)	2.86 / < 1.5
Pulse repetition rate (Hz)	14
Distance target station - detector (km)	540
FD fiducial volume (kt)	540

References :

[1] <https://essnusb.eu>

[2] <https://europeanspallationsource.se>

[3] M. Blennow et al, Eur. Phys. J. C **80** 190 (2020) [arXiv:1912.04309].

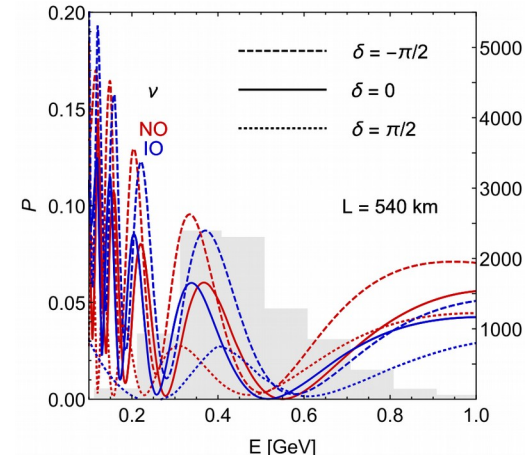
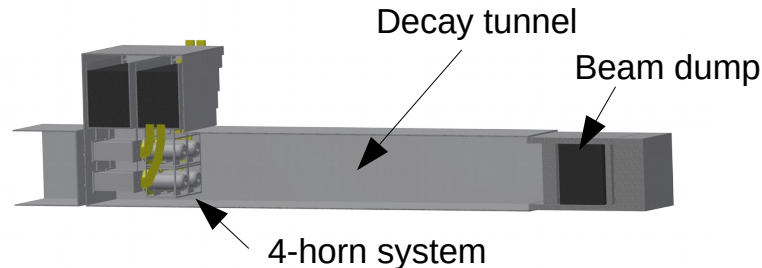


Fig. 2 : Oscillation probability as function of neutrino energy for different values of  $\delta_{CP}$ <sup>[3]</sup>

# The Target Station



The target station is made of three major elements : the hadron collector, the decay tunnel and the beam dump.

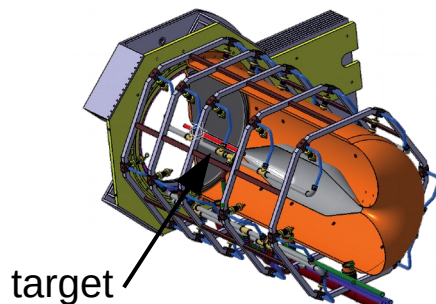


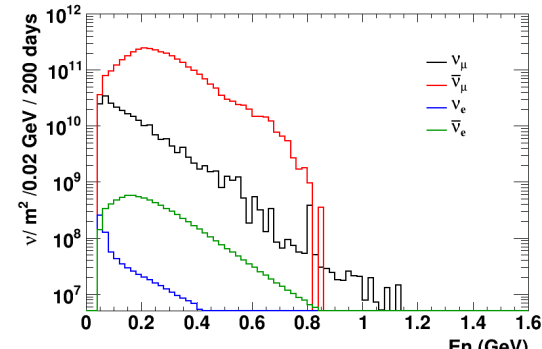
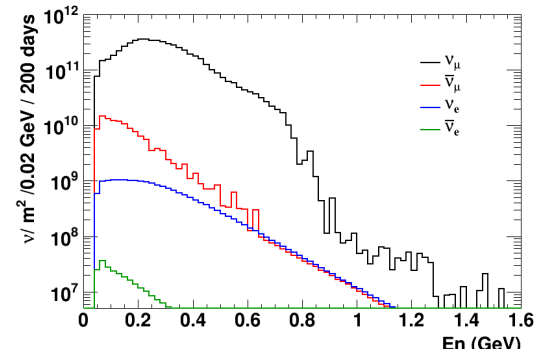
Fig. 3 : A magnetic horn<sup>[4][5]</sup>

## Hadron collector complex :

- 4 magnetic horn-target systems,
- 350 kA pulsed current,
- 2 focusing modes,
- Packed-bed targets : 3 mm diameter titanium spheres, 78 cm long, 1.5 cm radius.

**Decay tunnel** : 25 m long

**Beam dump** : one-block graphite (4\*4\*3.2 m<sup>3</sup>)



## References :

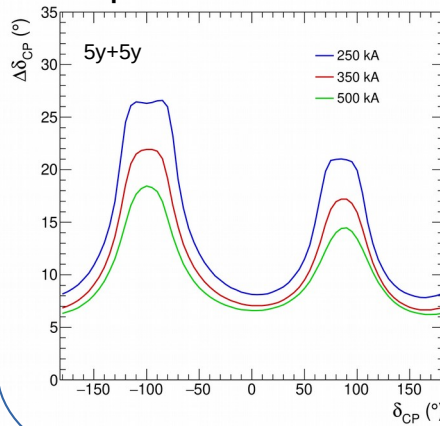
- [4] T. R. Edgecock et al, Phys. Rev. ST Accel. Beams **16** (2013), 021002, [arXiv:1305.4067 [physics.acc-ph]].
- [5] E. Baussan et al, Phys. Rev. ST Accel. Beams **17** (2014), 031001, [arXiv:1212.0732 [physics.acc-ph]].
- [6] L. D'Alessi, PoS, NuFact2019:062, 2020.

Fig. 4 : Neutrino fluxes as function of energy for a year of running time for positive and negative focusing respectively.<sup>[6]</sup>

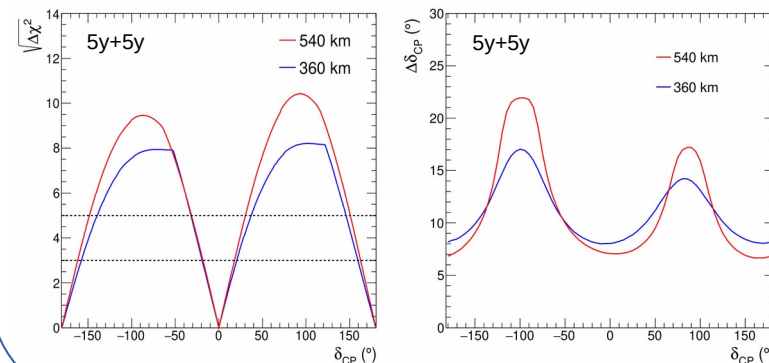
# A parameter study for physics optimization

Different studies have been done at the level of the target station facility and the magnetic horns in order to improve the sensitivity of ESSvSB for the measurement of  $\delta_{CP}$ .  $v$  fluxes were generated with Geant4<sup>[7][8][9]</sup> and sensitivity plots obtained with GLoBES<sup>[10][11]</sup>.

## 1. Influence of the current delivered to the horn on the performances.

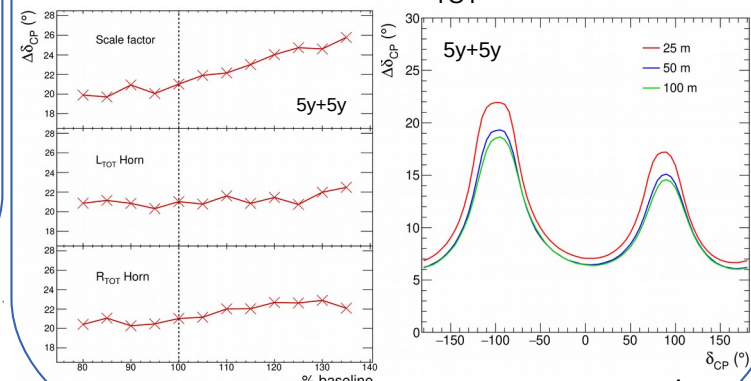


## 2. Influence of different baselines. There are two predominant choices : the mine of Garpenberg at 540 km and the mine of Zinkgruvan at 360 km.



## 3. A parametric study on the horn dimensions and the decay tunnel :

- Both total length and radius of the horn are modified (Scale Factor),
- Only the total length of the horn is modified ( $L_{TOT}$  Horn),
- Only the total radius of the horn is modified ( $R_{TOT}$  Horn).



References :

- [7] S. Agostinelli et al, Nucl. Instrum. Methods A 506, 250-303 (2002) DOI:10.2172/799992
- [8] S. Agostinelli et al, IEEE Trans. Nucl. Sci. 53, 70-278 (2006) DOI:10.1109/TNS.2006.869826
- [9] J. Allison et al, Nucl. Instrum. Methods A 835, 186-225 (2016) DOI:10.1016/j.nima.2016.06.125
- [10] P. Huber et al, Comput. Phys. Commun. **167** 195 (2005) [arXiv:hep-ph/0407333].
- [11] P. Huber et al, Comput. Phys. Commun. **177** 432–438 (2007) [arXiv:hep-ph/0701187].

# BACK UP

# 1. CP violation in leptonic sector

$$\begin{bmatrix} 1 & 0 & 0 \\ 0 & c_{23} & s_{23} \\ 0 & -s_{23} & c_{23} \end{bmatrix} \begin{bmatrix} c_{13} & 0 & s_{13}e^{-i\delta_{CP}} \\ 0 & 1 & 0 \\ -s_{13}e^{i\delta_{CP}} & 0 & c_{13} \end{bmatrix} \begin{bmatrix} c_{12} & s_{12} & 0 \\ -s_{12} & c_{12} & 0 \\ 0 & 0 & 1 \end{bmatrix} \\ = \begin{bmatrix} c_{12}c_{13} & s_{12}c_{13} & s_{13}e^{-i\delta_{CP}} \\ -s_{12}c_{23} - c_{12}s_{23}s_{13}e^{i\delta_{CP}} & c_{12}c_{23} - s_{12}s_{23}s_{13}e^{i\delta_{CP}} & s_{23}c_{13} \\ s_{12}s_{23} - c_{12}c_{23}s_{13}e^{i\delta_{CP}} & -c_{12}s_{23} - s_{12}c_{23}s_{13}e^{i\delta_{CP}} & c_{23}c_{13} \end{bmatrix}.$$

PMNS matrix

$$|U|_{3\sigma}^{\text{with SK-atm}} = \begin{pmatrix} 0.797 \rightarrow 0.842 & 0.518 \rightarrow 0.585 & 0.143 \rightarrow 0.156 \\ 0.243 \rightarrow 0.490 & 0.473 \rightarrow 0.674 & 0.651 \rightarrow 0.772 \\ 0.295 \rightarrow 0.525 & 0.493 \rightarrow 0.688 & 0.618 \rightarrow 0.744 \end{pmatrix}$$

	Normal Ordering (best fit)		Inverted Ordering ( $\Delta\chi^2 = 10.4$ )	
	bfp $\pm 1\sigma$	$3\sigma$ range	bfp $\pm 1\sigma$	$3\sigma$ range
$\sin^2 \theta_{12}$	$0.310_{-0.012}^{+0.013}$	$0.275 \rightarrow 0.350$	$0.310_{-0.012}^{+0.013}$	$0.275 \rightarrow 0.350$
$\theta_{12}/^\circ$	$33.82_{-0.76}^{+0.78}$	$31.61 \rightarrow 36.27$	$33.82_{-0.75}^{+0.78}$	$31.61 \rightarrow 36.27$
$\sin^2 \theta_{23}$	$0.563_{-0.024}^{+0.018}$	$0.433 \rightarrow 0.609$	$0.565_{-0.022}^{+0.017}$	$0.436 \rightarrow 0.610$
$\theta_{23}/^\circ$	$48.6_{-1.4}^{+1.0}$	$41.1 \rightarrow 51.3$	$48.8_{-1.2}^{+1.0}$	$41.4 \rightarrow 51.3$
$\sin^2 \theta_{13}$	$0.02237_{-0.00065}^{+0.00066}$	$0.02044 \rightarrow 0.02435$	$0.02259_{-0.00065}^{+0.00065}$	$0.02064 \rightarrow 0.02457$
$\theta_{13}/^\circ$	$8.60_{-0.13}^{+0.13}$	$8.22 \rightarrow 8.98$	$8.64_{-0.13}^{+0.12}$	$8.26 \rightarrow 9.02$
$\delta_{CP}/^\circ$	$221_{-28}^{+39}$	$144 \rightarrow 357$	$282_{-25}^{+23}$	$205 \rightarrow 348$
$\frac{\Delta m_{21}^2}{10^{-5} \text{ eV}^2}$	$7.39_{-0.20}^{+0.21}$	$6.79 \rightarrow 8.01$	$7.39_{-0.20}^{+0.21}$	$6.79 \rightarrow 8.01$
$\frac{\Delta m_{3\ell}^2}{10^{-3} \text{ eV}^2}$	$+2.528_{-0.031}^{+0.029}$	$+2.436 \rightarrow +2.618$	$-2.510_{-0.031}^{+0.030}$	$-2.601 \rightarrow -2.419$

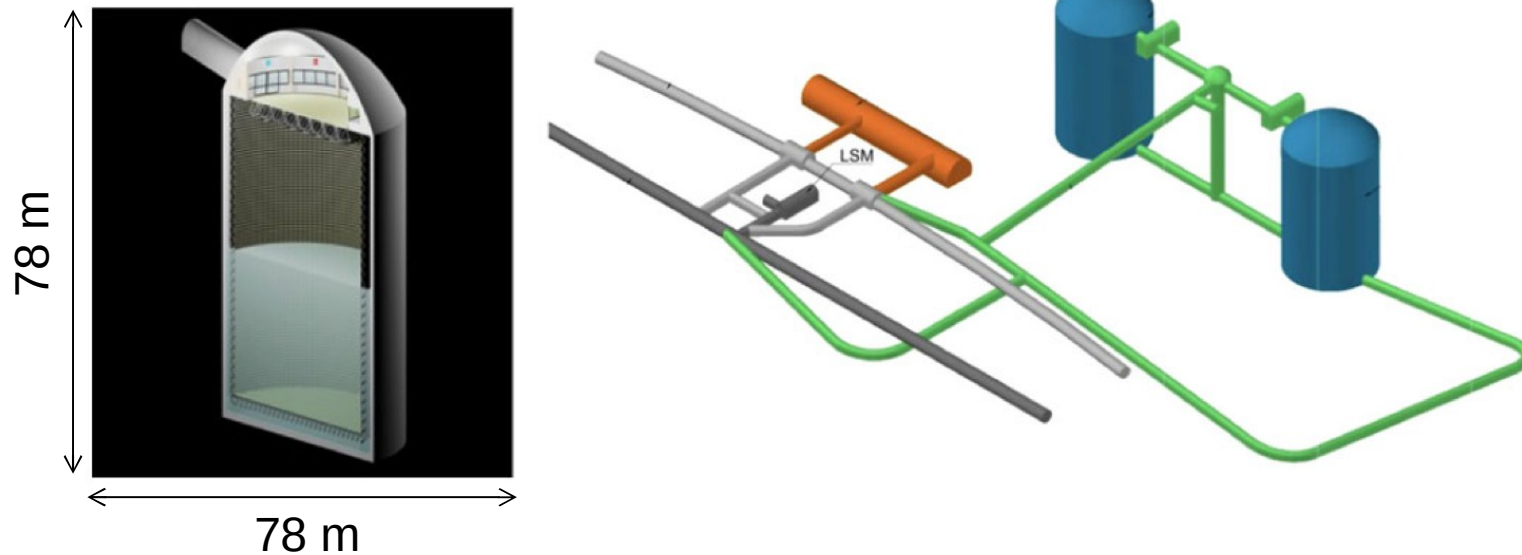
Current values of the PMNS matrix parameters<sup>[1][2]</sup>

References :

[1] I. Esteban et al. JHEP 01 (2019) 106 [arXiv:1811.05487]

[2] NuFIT 4.1 (2019), [www.nu-fit.org](http://www.nu-fit.org).

## 2. The ESSvSB project



Schematic view of a MEMPHYS module (left) and design for installation and infrastructure at a possible extension of the LSM underground laboratory at the Fréjus site<sup>[1]</sup>

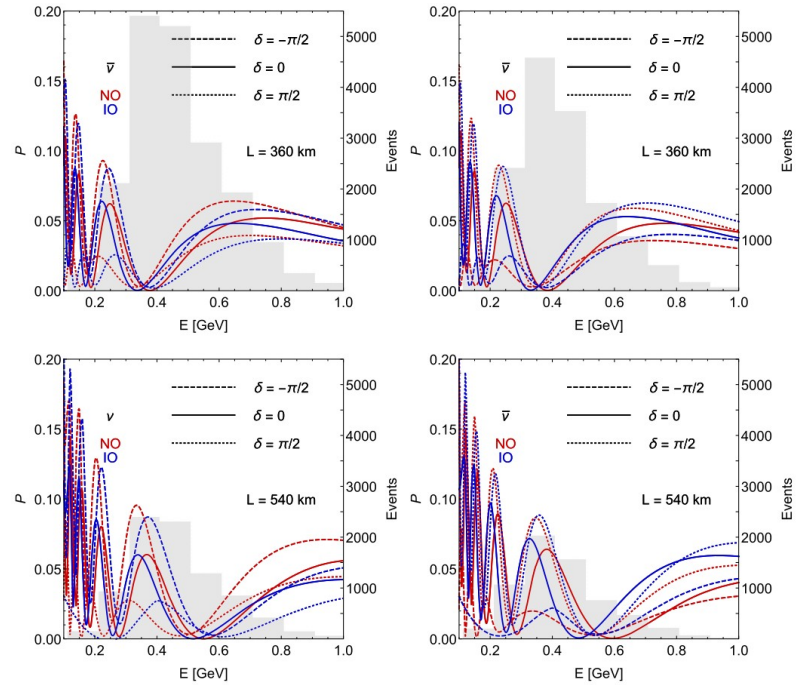
- 2 x 270 kt fiducial volume (~20xSuperK)
- Readout: 2x38k 20" PMTs
- 30% optical coverage

Reference :

[1] L. Agostino et al. Future large-scale water-cherenkov detector. Phys. Rev. ST Accel. Beams, 16:061001, Jun 2013



Possible sites for the far detector<sup>[1]</sup>



Oscillation probability as function of neutrino energy for different values of  $\delta_{CP}$  for different mines<sup>[2]</sup>

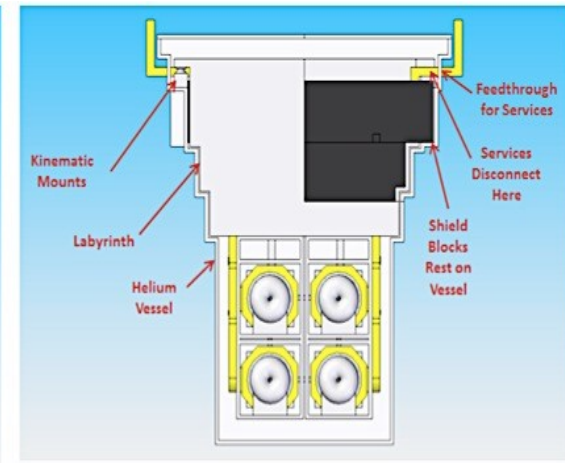
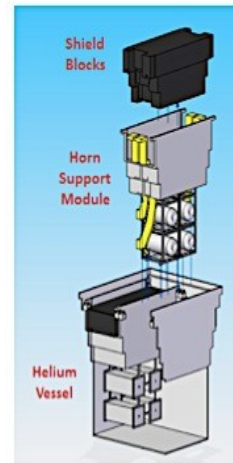
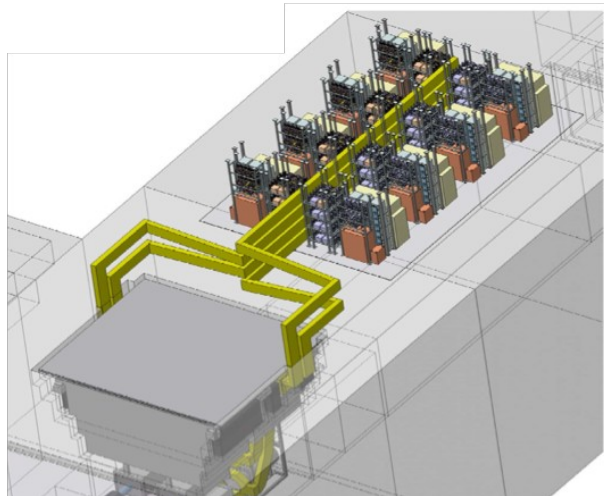
References :

[1] E. Baussan et al, Nuclear Physics B, Volume 885, 2014, Pages 127-149,

DOI :10.1016/j.nuclphysb.2014.05.016.

[2] M. Blennow et al, Eur. Phys. J. C **80** (3) 190 (2020) [arXiv:1912.04309]

# 3. The target station

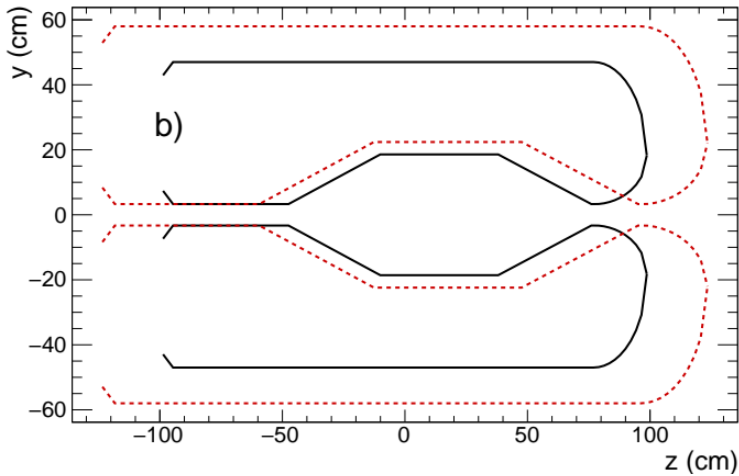


The power supply of the target station<sup>[1][2]</sup>

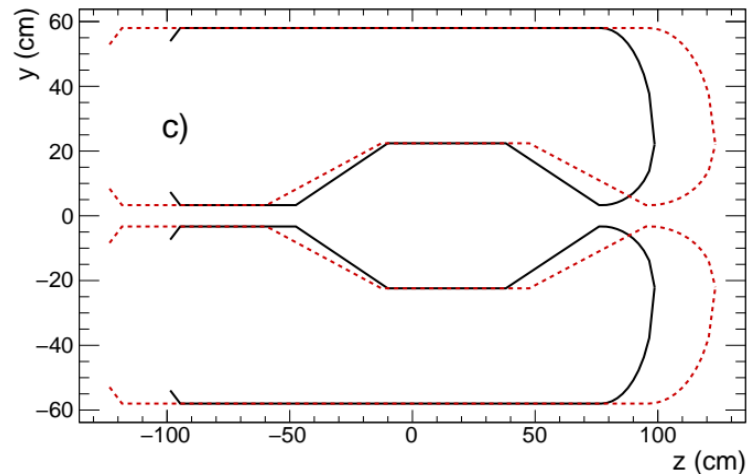
References :

- [1] T. R. Edgecock et al, Phys. Rev. ST Accel. Beams **16** (2013), 021002, [arXiv:1305.4067 [physics.acc-ph]].
- [2] E. Baussan et al, Phys. Rev. ST Accel. Beams **17** (2014), 031001, [arXiv:1212.0732 [physics.acc-ph]]

# 4. A parameter study for physics optimization

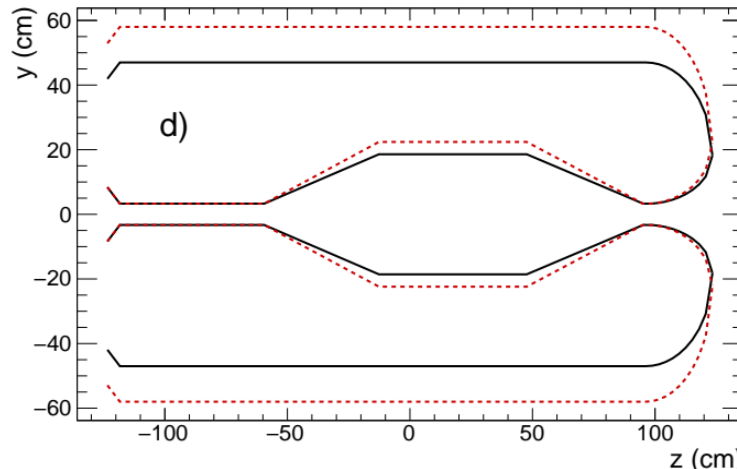


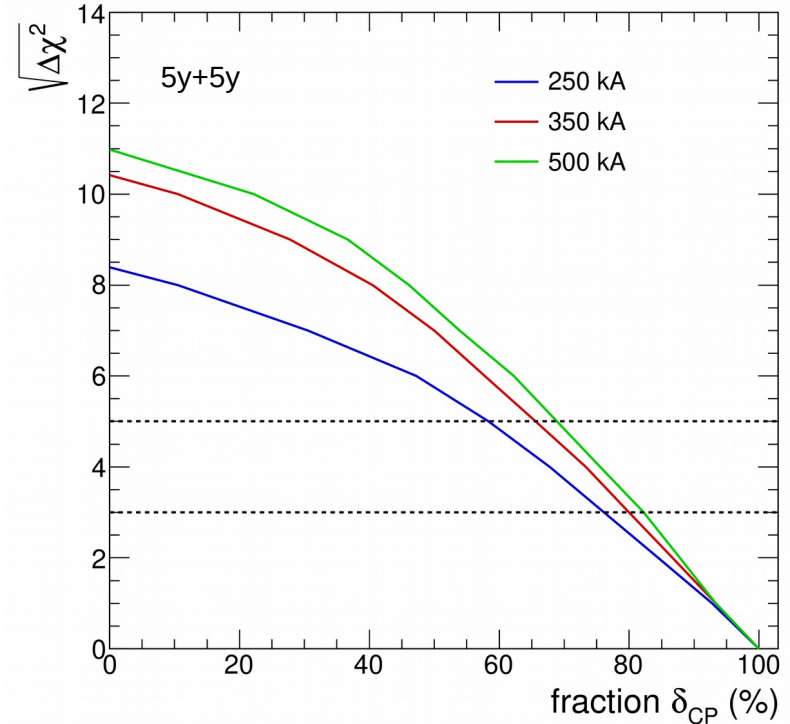
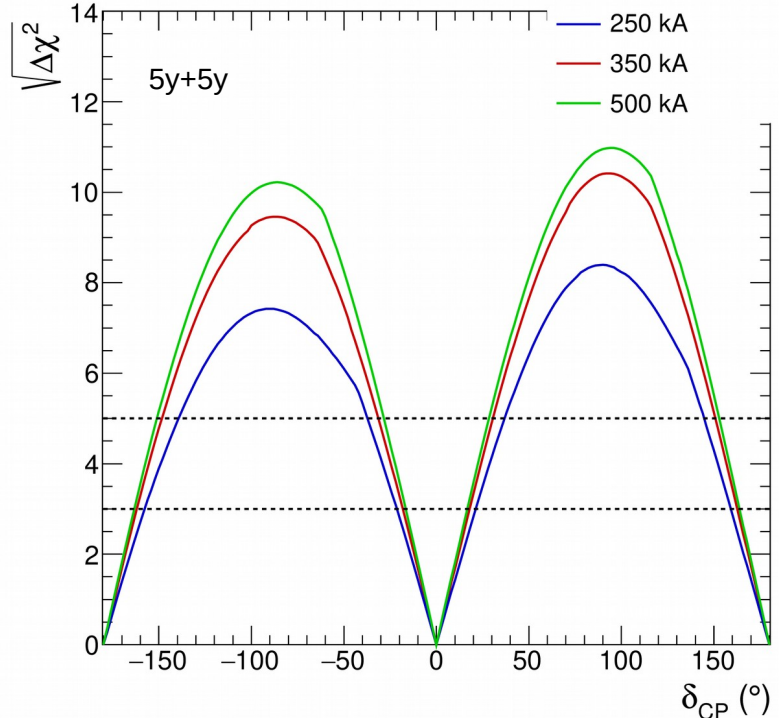
Scheme of the scale factor effect



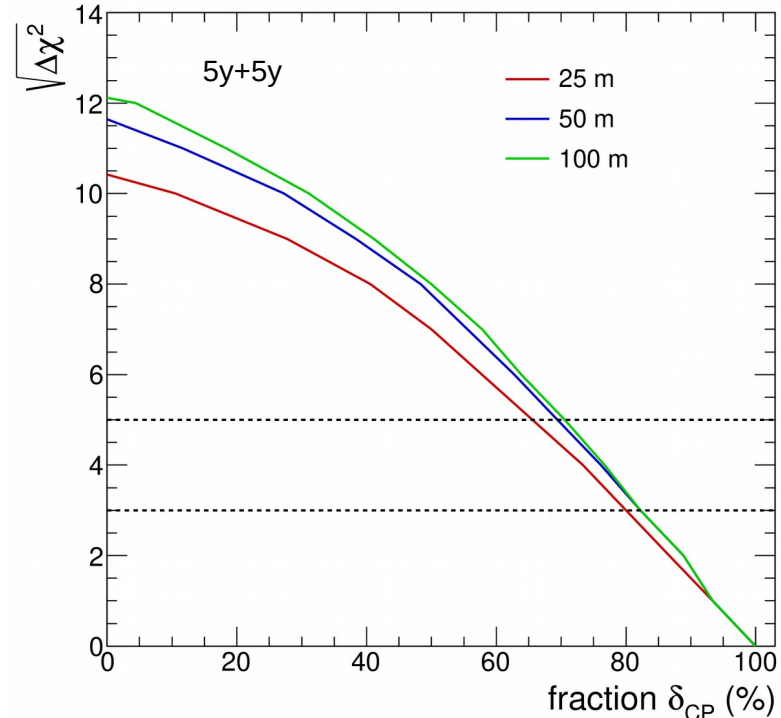
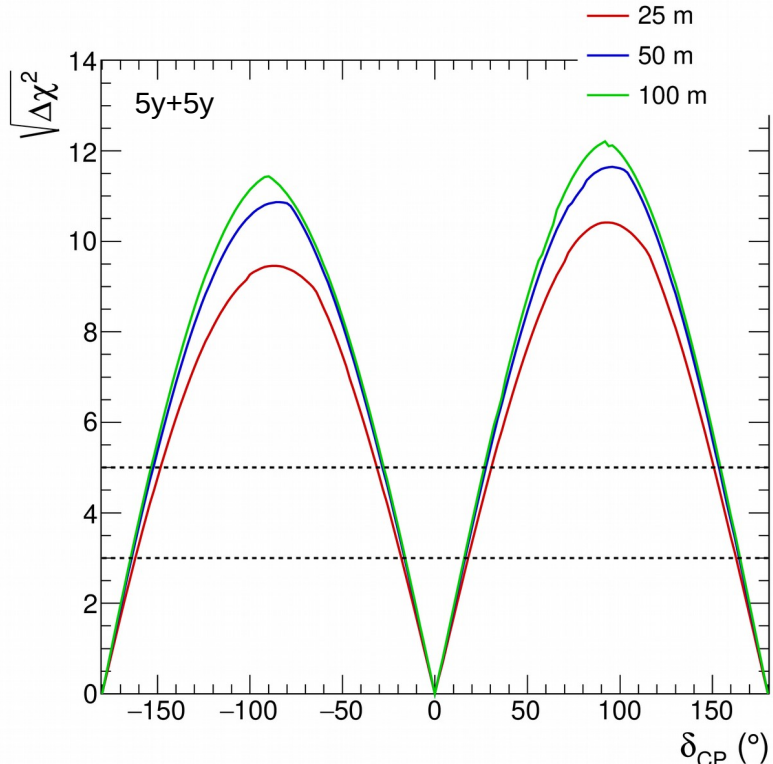
Scheme of the  $L_{TOT}$  parameter effect

Scheme of the  $R_{TOT}$  parameter effect

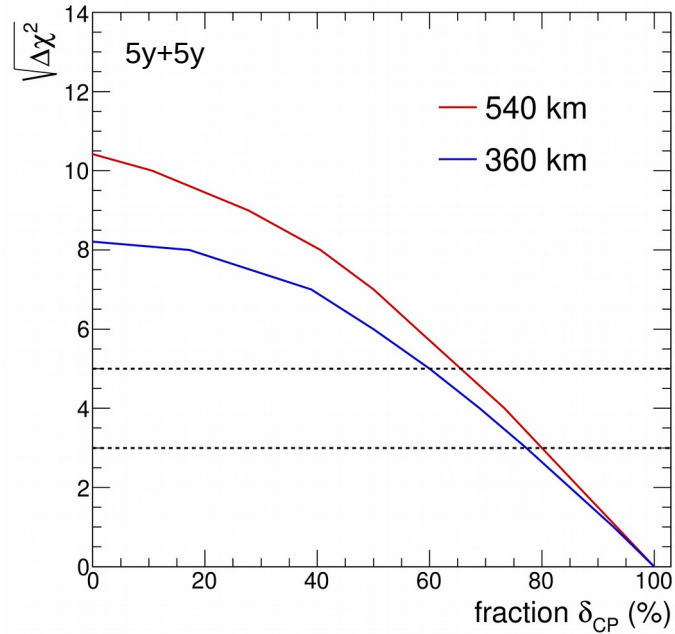




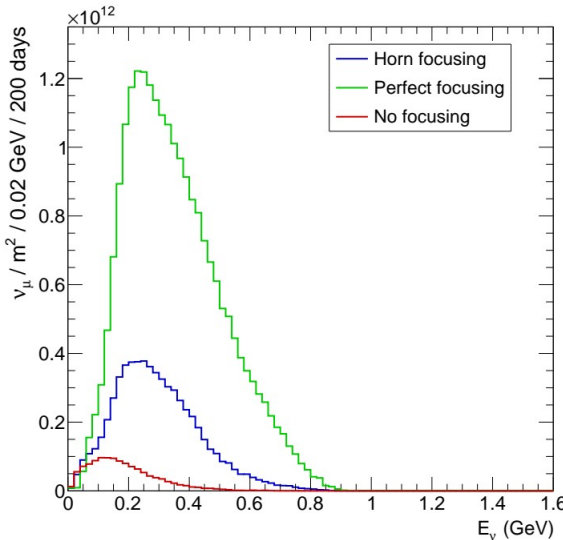
CP discovery potential at 540 km according to true values of  $\delta_{CP}$  (left) and fraction of delta covered (right) for different values of the current.



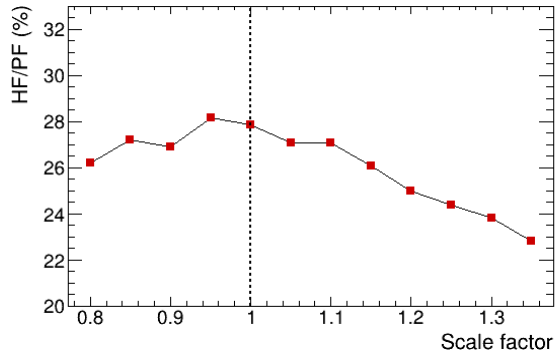
CP discovery potential at 540 km according to true values of  $\delta_{CP}$  (left) and fraction of delta covered (right) for different values of the decay tunnel length.



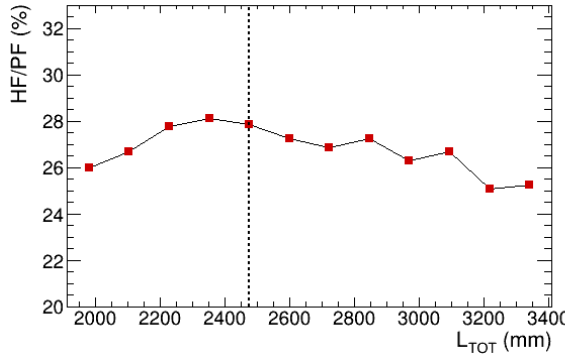
Fraction of delta covered for different baselines.



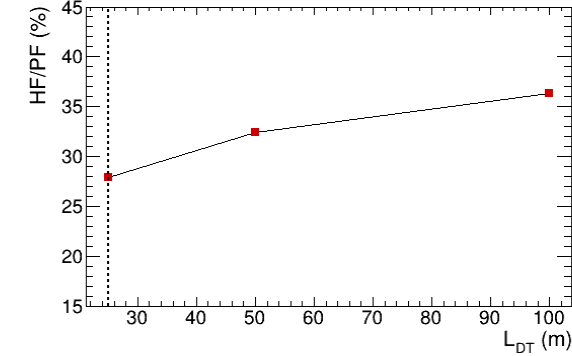
Evolution of the  $\nu$  flux according to the type of focusing



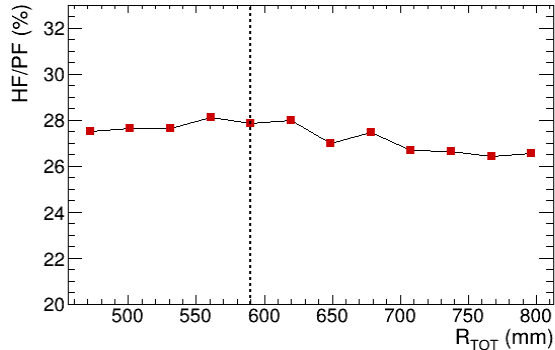
Evolution of the ratio Horn Focusing / Perfect Focusing according to the scale factor



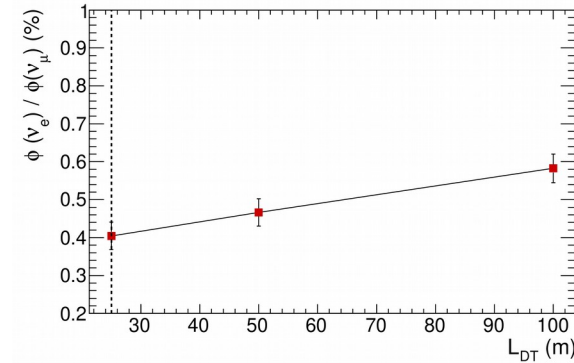
Evolution of the ratio Horn Focusing / Perfect Focusing according to  $L_{TOT}$



Evolution of the ratio Horn Focusing / Perfect Focusing according to the length of the decay tunnel



Evolution of the ratio Horn Focusing / Perfect Focusing according to  $R_{TOT}$



Evolution of the contamination of the  $\nu$  beam according to the length of the decay tunnel